Tabriz Journal of Electrical Engineering (TJEE), vol. 54, no. 4, December 2024 Serial no. 110
DOI: 10.22034/tjee.2023.57843.4683

# High Performance Hybrid Robust Extended Kalman Filter Design with Application to Large Misalignments

Fatemeh Rahemi, Mohammad Javad Khosrowjerdi*, Ahmad Akbari [1], Saeed Ebadollahi[2]

Faculty of Electrical Engineering, Sahand University of Technology, Tabriz, Iran[1]
Electrical Engineering, Department of Electrical Engineering, Iran University of Science and Technology, Tehran, Iran[2]
f.rahemi@sut.ac.ir, khosrowjerdi@sut.ac.ir, a.akbari@sut.ac.ir, s_ebadollahi@iust.ac.ir
P.O.Box: 51335-1996, Tabriz, Iran[1]

* Corresponding author

Received: Revised: Accepted:

**Abstract**
In many applications, especially military applications, the inertial navigation system (INS) needs to achieve a high level of accuracy in a short time. For alignment, recursive estimator filters and, in non-linear cases, the Extended Kalman Filter (EKF) is often used. The dynamics of a real, continuous system and the output of the sensors are available discretely. Therefore, a hybrid filter has been used. In addition, a robust filter is used to increase the reliability of system operation. In this paper, a Hybrid Extended Kalman Filter (HEKF) is presented and then upgraded to the Hybrid Robust Extended Kalman Filter (HREKF). By running the algorithm on the data of a real system, it was observed that the speed of convergence increased especially in the yaw direction. By running the algorithm on the data of a real system, it was observed that the speed of convergence has increased especially in the yaw direction. Finally, using the impulsive system approach, a new stability analysis of the proposed algorithms is presented, which guarantees the boundedness of the error estimation, which is unique.

**Keywords**
*Dual Estimation, Hybrid Extended Kalman Filter, Hybrid Robust Extended Kalman Filter, Large Misalignments*

## 1. Introduction

In many applications, such as Unmanned Aerial Vehicle (UAV) navigation [1, 2], mobile devices [3], Autonomous Underwater Vehicle (AUV) navigation [4], and human body motion tracking [5], etc., especially military applications, the inertial navigation system needs to achieve a high level of accuracy in a short time [6].

Alignment means finding the connection between the physical coordinate system, and the navigation device [7, 8] which is very important in the navigation process. Converting the sensor readings into the reference frame's height, velocity, and starting position requires an accurate orientation calculation. Poor initial levels cause poor navigation. Navigation systems that only work with low-cost Micro Electro Mechanical System (MEMS) sensors quickly diverge [9]. The system is based on the output of the gyroscope sensor, which is updated by gravitational and magnetic sensors.

Kalman Filter (KF) and Extended Kalman Filter (EKF), as the most well-known and widely adopted approaches, were applied in diverse areas, especially in the orientation estimation [9-12]. In recent years, estimation algorithms based on navigators integrated for various land, sea, and air systems have been widely developed. One of the most common algorithms for estimation is the Kalman filter. In solving navigation problems, the Kalman filter is used in linear models with Gaussian noise, and the EKF is used in linear models with non-Gaussian noise. [13].Moreover, the Robust Extended Kalman Filter (REKF) was considered for nonlinear systems by researchers [14, 15].

For example, two covariance-tuning methods to form a Robust Kalman Filter (RKF) algorithm for attitude (i.e., roll and pitch) estimation using the measurements of only an Inertial Measurement Unit (IMU) have been proposed by Candan et al. [16]. Both of the proposed methods include an adaptive mechanism for modifying the measurement noise covariance to provide reliable estimates of the two axes of orientation. For nonlinear systems, additional approaches have been utilized, such as observer design [17].

Regarding a low-cost Inertial Measurement Unit (IMU), an orientation estimation strategy for a non-accelerated platform was presented. Kalman filter is the most used technique to solve the problem of initial alignment [18]. However, it can only deal with initial alignment under small misalignment angles. Under large initial azimuth misalignment angle conditions, the model of SINS is nonlinear, and it could be processed by nonlinear filtering. Large misalignment angles and uncertain noise are two main problems in initial alignment in different application environments [19]. The nonlinear model of SINS and nonlinear methods are developed to solve the alignment problem. The widely used nonlinear filtering method in engineering is EKF [20].

An EKF's performance may be significantly harmed by linearization faults that are inherent in the specification. In practice, the EKF has performance limitations. One of these limitations is considering process noise and Gaussian measurement. This assumption is not always true. Therefore, this problem can seriously affect the performance

DOI: 10.22034/tjee.2023.57843.4683

of the algorithm or even lead to a deviation in the estimation. [21]

On the other hand, SINS initial alignment with unknown noise, the conventional nonlinear filtering approach discussed above will result in a larger estimate error if the environment noise is not Gaussian white noise. In recent years, the combination of magnetometer data, and inertial sensors was widely used in estimating the situation [22, 23]. The data from the gyroscope is integrated to obtain the orientation, while the data from the accelerometer and magnetometer are used to estimate the gyroscope biases online. However, the estimation accuracy of the two methods depends on the accelerometer and magnetometer. In the proposed method, the quaternion associated with the bias of the accelerometer and magnetometer is modelled as the state vector to estimate the bias of the gyroscope for online calibration [22].

For practical systems, the hybrid model is more compatible with considering implementation restrictions. In this paper, a hybrid algorithm is presented because previous algorithms were unable to provide an accurate estimate for the yaw in practical implementations of SINS. A hybrid system is a dynamic system with continuous and discrete dynamic behavior. A hybrid system has the benefit of encompassing a larger class of systems within its structure, allowing for more flexibility in modeling dynamic phenomena [8]. As far as the authors have investigated, no research work has been done regarding HREKF and algorithm design and stability proof and simulation with real data, and this is the important innovation of this article.

The difference between this article and other research is; Presenting the new HREKF algorithm, proving the stability and convergence of that algorithm, and practical system implementation. HREKF could achieve the results at a significantly lower expense than HEKF, and obtain a high accuracy even when the statistical property of noise is uncertain, or the outliers of measurement occasionally occur. As can be observed from the findings, the HREKF outperforms the other filters, particularly in the YAW direction, since it is resistant to process and system noise as well as unknown inputs and different kinds of uncertainties. The results show that the proposed algorithm performs more efficiently than other observers to ensure the yaw direction and eliminate perturbation in addition to the less structural complexity.

Considering that the evaluation and adaptation of the HREKF method to the specific requirements and characteristics of the target system have been important for ensuring optimal results, the Lipchitz condition has played a crucial role in checking nonlinear systems when applying this method in other systems. This algorithm has received favorable responses for a real critical operating system, indicating its effectiveness. Furthermore, the aforementioned mathematical condition has proven valid for a wide range of real systems. Consequently, this method has demonstrated versatility and can be employed in similar applications without specific systematic limitations.

The article is organized as follows. After explaining the problem, HEKF is presented in algorithm 1 and HREKF in algorithm 2, and the differences between the two algorithms are shown. After that, the stability of HREKF has been analyzed, and in the next step, with real data, the efficiency of HREKF has been shown in this particular field, and as a result, it clearly shows that the HREKF algorithm works better than HEKF.

## 2. Problem Formulation and Designed Algorithms

Motivated by the idea of hybrid systems, two kinds of HEKF are given. The dynamic of the system is continuous, where the measurement is discrete. The considered nonlinear hybrid system in this paper is represented by

$$\dot{x} = f(x,u,t) + \omega(t) \qquad \omega(t) \sim (0,Q) \qquad (1)$$
$$y_k = h_k(x_k) + \nu_k \qquad \nu_k \sim (0,R_k)$$

where $x \in \mathbb{R}^m$ , $y_k \in \mathbb{R}^n$ $u \in \mathbb{R}^\ell$ denote the state, measurement vectors, and control input respectively. The nonlinear function $f(\cdot)$ is assumed to be continuously differentiable and $h_k$ is the measurement. $\omega(t)$ and $\nu_k$ are uncorrelated zero mean white noise processes with covariance matrices $Q$ and $R_k$ respectively. Since dual estimation is done in this article, the process noise covariance is divided into two general parts. In cases where we have parameter estimation, the covariance matrix can be recursively estimated with Robbins-Monroe coefficients in each step and increase the modeling accuracy. $\bar{Q}$ is the variance of process noise. $Q_{\omega_k}$ is the part of the covariance matrix of the process noise that estimates with Robbins-Monro coefficients, and $\bar{Q}$ is a constant part.

$$Q = \begin{bmatrix} \bar{Q} & 0 \\ 0 & Q_{\omega_k} \end{bmatrix}$$

The gyroscope output is used to predict the direction during propagation, which is known as the previous estimate. Kalman filter-based algorithms consist of two crucial processes: time update and measurement update. During measurement updates, the magnetometer and accelerometer outputs are utilized to correct the previous estimate, resulting in a posterior estimate.

The paper continues by presenting an experimental implementation of a real SINS, where the HREKF algorithm is used to estimate the situation using angular velocity measurements from a gyroscope and a measurement vector. The algorithm aims to achieve convergence in estimating the state matrix and bias estimation of the gyroscope to actual values. To rectify the inaccuracies in YAW angle calculation, the magnetometer is utilized since it has higher precision. Combining the accelerometer with the magnetometer eliminates the output data drift of the gyroscope. By integrating the output of the gyroscope and combining it with information from the accelerometer and magnetometer sensors, more precise position angles can be obtained. In the HEKF framework, which is designed for nonlinear systems, the systems operate continuously and the measurements are discrete. In the continuous part, the measurements (Gyro Measurements) are discrete but they are considered constant in time intervals. For this reason, mixed modelling was done. Therefore, the system consists of two parts, continuous and discrete. In this paper, HEKF and HREKF are presented as Algorithm 1 and Algorithm 2.

Algorithm 1 is an improved algorithm presented by Dan Simon [24]. Kalman filters are highly sensitive to system

DOI: 10.22034/tjee.2023.57843.4683

modelling. For this reason, the covariance of the process noise, which indicates the accuracy of the modelling, becomes more accurate at each step. Parameter estimation is performed at each step.

In Step 3, $Q_{\omega_k}$ is estimated based on the Robbins-Monro stochastic approximation method [24]. Due to differences between environment noises and the variety of properties of noise, the covariance matrix is estimated continuously in this method which yields a more accurate model of the real system.

In the above algorithm, $M_k$ is the mean state estimate matrix of the previous step which can be considered as a constant in all steps.

HEKF makes the accurate knowledge dynamic model of the system under consideration one of its basic tenets. Since the filter type may not be resistant to this uncertainty, further techniques were created with the same objective in mind, and a discrete-time state estimator was created. The approach taken in the robust HEKF is not to neglect the higher-order terms of Taylor series expansions but rather to assume them to be functions of the state estimation error and the exogenous inputs that have bounded $H_\infty$. This approach leads to a minimax estimation problem that can be treated using standard $H_\infty$ methods.

Since the equations of the system are continuous and the measurements are discrete, then the filters must be hybrid. So we have two time parameters, T is sample time and dt is the step size and time interval used to solve the continuous part. Algorithm 1 is presented as follows.

**Algorithm 1. Hybrid Extended Kalman Filter**

**Step 1:** Initialization

Initialize arbitrary value for $\hat{x}_0^+$ and $P_0^+$ as follows

$\hat{x}_0^+ = E[x_0]$

$P_0^+ = E[(x_0 - \hat{x}_0^+)(x_0 - \hat{x}_0^+)^T]$

**Step 2:** Time Update (Prediction Cycle)

Predict $\hat{x}$ by using the following one step ahead state prediction formula:

$\hat{x}_k^- = \hat{x}_{k-1}^+ + dt(f(\hat{x}_{k-1}^+, u_{k-1}, \omega_{k-1}, k-1))$

Predict $P$ by using the following one step ahead error covariance matrix prediction:

Recursive formula: $P_k^- = P_{k-1}^+ + dt(F_k P_{k-1}^+ + P_{k-1}^+ F_k^T + L\mathrm{Q}_k L^T)$

**Step 3:** Measurement Update (Correction Cycle)

Update covariance matrix $Q_{\omega_k}$ as follows (Robbins-Monroe stochastic approximation)

$\mathrm{Q}_{\omega_k} = (1-\alpha)Q_{\omega_{k-1}} + \alpha k_k\big(y_k - h(\hat{x})\big)\big(y_k - h(\hat{x})\big)^T k_k^T \qquad 0 \le \alpha \le 1$

$Q_k = \begin{bmatrix} \bar{Q} & 0 \\ 0 & \mathrm{Q}_{\omega_k} \end{bmatrix}$

Obtain Kalman Gain as follows

$K_k = P_k^- H_k^T (H_k P_k^- H_k^T + M_k R_k M_k^T)^{-1}$

Update state estimate as follows

$\hat{x}_k^+ = \hat{x}_k^- + K_k\big(y_k - h_k(\hat{x}_k^-, 0, t_k)\big)$

Update the error covariance matrix as follows

$P_k^+ = (I - K_k H_k) P_k^- (I - K_k H_k)^T + K_k M_k R_k M_k^T K_k^T$

where the Jacobean matrix of $f(x_{k-1})$ and $h(x_k)$ are obtained as

$F_k = \left.\frac{\partial f(x)}{\partial x}\right|_{\hat{x}_k}$

$H_k = \left.\frac{\partial h(x)}{\partial x}\right|_{\hat{x}_k}$

$M_k = \left.\frac{\partial h}{\partial v}\right|_{\hat{x}_k}$

$L_k = \left.\frac{\partial f(x)}{\partial \omega}\right|_{\hat{x}_k}$

where $I$ Represent the identity matrix.

The HEKF is obtained by first-order linearization of the nonlinear model, and the approximation error between the linear model and the original nonlinear system may be significant. In this case, there are many deviations of the estimated state from the actual state. Linearization error reduction by modelling these errors in uncertainty makes the system equations more accurate. To increase the reliability of the system and guarantee of boundedness of the estimation error, a novel method is proposed to design the HREKF

The main purpose of HREKF design is to guarantee the norm of the transfer function among the external disturbances (modeling errors and system noises), and the estimation error to be less than a prescribed attenuation level $\gamma$ which satisfies $\frac{\|e_k\|^2}{\|\omega_k\|^2+\|\Delta_k\|^2+\|v_k\|^2} \le \gamma^2$ where $e_k$ is the estimation error ($e_k = x_k - \hat{x}_k$), $\omega_k$ and $v_k$ are the noise

DOI: 10.22034/tjee.2023.57843.4683

vectors and $\Delta_k = f(x,u,t) - f(\hat{x},u,t) - F_k e_k$ is the model error caused by unknown exogenous inputs or by linearization error. Tuning of attenuation level implies that the ability of the HREKF to minimize the energy of the estimation error is limited by the maximum eigenvalue of $P_k^-$ . For a fixed value of $\gamma$ the bound of the estimation error $\|e_k\|^2$ is enlarged by the presence of a linearization error or unknown exogenous inputs. The tuning parameter $\gamma$ is nonzero and is set to maintain $\Sigma_{k|k-1}$ as a positive definite matrix. The structure of HREKF is similar to HEKF when $\gamma = \infty$.

Additionally, a significant difference between the projected state and the actual state will raise the linearization error. The filter will not converge if this tendency is not reversed. The result shows that a nonlinear robust filter is more stable than HEKF and can effectively improve the accuracy of initial alignment, and the robustness of the algorithm. We will derive the HREKF, which considers systems with continuous time dynamics. This is the most common situation encountered in practice. In this experiment, we have a continuous time with discrete time. Algorithm 2 gives a design procedure for HREKF As follows.

**Algorithm 2. Hybrid Robust Extended Kalman Filter**

**Step 1:** Initialization:

Initialize arbitrary value for $\hat{x}_0^+$ and $P_0^+$ as follows

$\hat{x}_0^+ = E[x_0]$

$P_0^+ = E[(x_0 - \hat{x}_0^+)(x_0 - \hat{x}_0^+)^T]$

**Step 2:** Time Update (Prediction Cycle)

Predict $\hat{x}$ by using the following one step ahead state prediction formula

$\hat{x}_k^- = \hat{x}_{k-1}^+ + dt(f(\hat{x}_{k-1}^+, u_{k-1}, \omega_{k-1}, k-1))$

Update the covariance matrix by the following one step ahead error covariance matrix prediction:

$P_k^- = P_{k-1}^+ + dt(F_k P_{k-1}^+ + P_{k-1}^+ F_k^T + L\mathrm{Q}_k L^T)$

One step ahead covariance matrix prediction:

$\Sigma_k^- = ((P_k{}^-)^{-1} - \gamma^{-2} L_k^T L_k)^{-1}$

**Step 3:** Measurement Update (Correction Cycle)

Define an auxiliary matrix as follows

$P_y = H_k \Sigma_k^- H_k^T + R_k$

Define the Kalman Gain estimate as follows

$K_k = \Sigma_k H_k^T P_y^{-1}$

Estimate state as follows:

$\hat{x}_k^+ = \hat{x}_k^- + K_k[y_k - h(\hat{x}_k^-)]$

The final estimation of the error covariance matrix is given by:

$P_k^+ = (\Sigma_k^{-1} + H_k^T R_k^{-1} H_k)^{-1}$

where the Jacobean matrix of $f(x_k)$ and $h(x_k)$ are obtained as) Discrete continuous.)

$F_k = \frac{\partial f(x)}{\partial x}\Big|_{\hat{x}_k}$

$H_k = \frac{\partial h(x)}{\partial x}\Big|_{\hat{x}_k}$

$L_k = \frac{\partial f(x)}{\partial \omega}|_{\hat{x}_k}$

where $I$ Represent the identity matrix.

**Remark 1:** The tuning parameter $\gamma$ in Step 3 is nonzero which is set to maintain $\Sigma$ a positive definite matrix. The norm of the transfer function of the estimation error is less than the attraction level $\gamma$. Tuning of the attenuation level implies that the ability of the HREKF to minimize the energy of estimation error is limited by the maximum eigenvalue of $P_k^+$ . Moreover, a large deviation of the estimated state from the real one will increase the linearization error. If this tendency does not stop, the filter will not converge.

## 3. Stability Analysis of HREKF

This section presents the stability analysis of HREKF. Inspired by the stability analysis method for impulsive systems, certain conditions are provided. The aim of proving stability is to demonstrate that the error converges to zero and remains at zero.

Define the error $e = x - \hat{x}$ yields

$$\dot{e} = \dot{x} - \dot{\hat{x}} = f(x,u,t) - f(\hat{x},u,t) \qquad (2)$$

As mentioned in the given algorithms, measurements are given at time $t_k$, and $\hat{x}$ is modified as follows:

DOI: 10.22034/tjee.2023.57843.4683

$$\hat{x}(t_k^+) - \hat{x}(t_k^-) = k_k(y_k - h(\hat{x}(t_k^- \quad (3)$$

So, the error value at time $t_k$ has a discrete change which is calculated from the following formula:

$$\begin{cases} e(t_k^+) = x(t_k^+) - \hat{x}(t_k^+) \\ e(t_k^-) = x(t_k^-) - \hat{x}(t_k^-) \end{cases} \quad (4)$$

where $e\,(t_k^+) - e(t_k^-) = x(t_k^+) - \hat{x}(t_k^+) - x(t_k^-) + \hat{x}(t_k^-)$. Here, $t_k^-$ and $t_k^+$ indicate before and after $t_k$. Since the dynamics of the system are continuous, then:

$$\Delta\big(e_k(t_k)\big) = e(t_k^+) - e(t_k^-) = K_k\left(y_k - h\big(\hat{x}(t_k^-)\big)\right) \quad (5)$$

We consider the noises as additive, so the error dynamics can be rewritten as the following stochastic impulsive system

$$\begin{cases} \dot{e}(t) = f(x,u,t) \;\; - f(\hat{x},u,t) & t \neq t_k \\ e(t_k^+) = e(t_k^-) - K_k\left(y_k - h\big(\hat{x}(t_k^-)\big)\right) & t = t_k \end{cases} \quad (6)$$

Impulsive time sequence $\mathcal{T} = \{t_1, t_2, \cdots\}$ is strictly increasing, and approaches to infinity. The function $f(x,u,t)$ is assumed to be continuous with respect to $t, x, u$ and uniformly locally Lipschitz with respect to $x, u$ $f(\cdot,0,0) = 0$. The function $h(\cdot)$ is discrete with respect to $x$. Assume that given an initial condition, there is a unique stochastic process satisfying the system (6).

Now, the following definitions and theorem give a sufficient condition to guarantee the stochastic system stability and boundedness of the error function.

**Definition 1**: Given an impulsive time sequence T, the impulsive stochastic nonlinear system (6) is stochastic input-to-state stability (SISS), if, for an arbitrary $\epsilon \in (0\ 1)$, there exist $\beta \in KL, \gamma \in K_\infty$ such that for all $x(t_0) \in \chi, u \in U. P\{|x(t)| \leq \beta(|x(t_0)|, t - t_0) + \gamma\|u\|\} \geq 1 - \epsilon\ \forall t \in R_{t^+}$

Here, P denotes to probability measure. Given a set S of admissible impulsive time sequences, if the system is SISS for every T$\in$ S and $\beta$, $\gamma$ does not depend on the choice of T, then the system (6) is uniformly SISS over S. KL and $K_\infty$ denote functions of class KL and $K_\infty$, respectively. [25]

**Definition 2:** Given an impulsive time sequence $T$, the impulsive stochastic nonlinear system (6) is stochastic global stability (SGS), if for an arbitrary $\epsilon \in (0\ 1)$, is exist $\gamma_1, \gamma_2 \in K_\infty$ such that for all $x(t_0) \in \chi, u \in U$.

$P\{|x(t)| \leq \gamma_1(|x(t_0)|,) + \gamma_2\|u\|\} \geq 1 - \epsilon \quad \forall t \in R_{t^+}$

Given a set S of the admissible impulsive time sequences, if the system is stochastic global stability (SGS) for every $T \in$ S and $\gamma_1, \gamma_2 \in K_\infty$ do not depend on the choice of $T$, then the system (6) is uniformly SISS over S. [25]

**Theorem 1:** Consider the stochastic nonlinear system (6) with Kalman gain $K_k = P\Sigma_k H_k^T$.

where $\Sigma_k^- = ((P_k{}^-)^{-1} - \gamma^{-2}L_k^T L_k)^{-1}$

If there exists a positive matrix $P$ and positive scalars $\epsilon, \delta, d$, and $c$ such the following conditions are met for all $a > 0$

$$\begin{bmatrix} (e^{-d} - 1)P & P\Sigma_k H_k^T P_y^{-1} & I \\ \left(\Sigma_k H_k^T P_y^{-1}\right)^T P^T & \epsilon^{-1} I & 0 \\ I & 0 & \epsilon\eta^{-1} I \end{bmatrix} > 0 \quad (7-a)$$

$$\int_a^{\psi(a)} \frac{ds}{\varphi(s)} \leq T - \delta \quad (7-b)$$

Then, system (6) is stochastically globally stable.

Here, T is the minimum time between two measurements, and $\varphi\big(V(e,t)\big)$ represents a function that is continuous and zero at zero. In the above relations $V(e,t): \chi \times \mathbb{R}_{t_0}^+ \to \mathbb{R}^+$ is an optional SISS-Lyapunov function and scalar $\eta$ has been gained from Lipshitz condition $\big(y - h(t_k^{-1})\big)^T \left(y - h\big(x(t_k)\big)\right) \leq \eta e(t)^T e(t)$. Matrices $P_y$, $\Sigma_k$, and $H_k^T$ have been defined in Algorithm I, previously.

In stochastic impulsive systems, as mentioned in the [26] (readers are referred to as Theorem 3.1 in Ref. [26]), we can always have an estimate of the function $E\|x(t)\|^p$ for the system.

Proof: See Appendix A.

**Remark 2**: In the above theorem, the Lyapunov function $V(e,t) = \frac{1}{2}e^T P e$ is considered which satisfies $\mathcal{L}V(e,t) \leq -\varphi\big(V(e,t)\big)$, and it is assumed $\big(y - h(t_k^{-1})\big)^T \left(y - h\big(x(t_k)\big)\right) \leq \eta e^T e$. Since the continuous dynamic system is stable, so we can get $\varphi\big(V(e,t)\big) = cV(e,t)$ where $c > 0$ and then $T > -\frac{d}{c} + \delta$ in which $\delta > 0$. Also, $\big(y - h(t_k^{-1})\big)^T \left(y - h\big(x(t_k)\big)\right) \leq \eta e^T e$ is concluded from the Lipchitz condition and $\eta$ is a positive scalar.

## 4. Experimental Implementation

This section presents the system equations for the experimental implementation of true SINS using the HREKF and HEKF methods. The attitude and bias are estimated using these methods, and the covariance of system error is continuously updated with reality. First, the equations of the system are presented, and then the results of HREKF and HEKF are presented to estimate attitude and bias.

### 4.1. System description

The state vector includes quaternions and bias gyroscopes, which are estimated at each step using recursive algorithms, defined as follows.

$$x = [q_0 \quad q_1 \quad q_2 \quad q_3 \quad \omega_{xb} \quad \omega_{yb} \quad \omega_{zb}]^T \quad (8)$$

where $\omega = [\omega_x \quad \omega_y \quad \omega_z]$ $q = [q_0 \quad q_1 \quad q_2 \quad q_3]$

Now, we develop HEKF for the specified SINS. As mentioned previously, the HEKF is the nonlinear version of the conventional Kalman Filter, which linearizes an estimate of the present state and covariance using the Jacobians of the prediction and measurement functions. This allows a whole new set of prediction and measurement models to be used for estimation, as long as the prediction, and measurement

DOI: 10.22034/tjee.2023.57843.4683

models $f$ and $h$ can be defined as differentiable functions of $x$.

The next quaternion is found through numerical integration using $q_k = q_{k-1} + dt * \dot{q}_k$ where

$$\dot{q}(q,\omega) = \frac{1}{2}\begin{bmatrix} -q_1 & -q_2 & -q_3 \\ q_0 & q_3 & -q_2 \\ -q_3 & q_0 & q_1 \\ q_2 & -q_1 & q_0 \end{bmatrix}\begin{bmatrix} \omega_x - \omega_{xb} \\ \omega_y - \omega_{yb} \\ \omega_z - \omega_{zb} \end{bmatrix} \quad (9)$$

The gyroscope biases are unchanged during the prediction step. This allows $f$ to be built as

$$x = \begin{bmatrix} q_0 + \frac{dt}{2} * \left(-q_1(\omega_x - \omega_{xb}) - q_2\left(\omega_y - \omega_{yb}\right) - q_3(\omega_z - \omega_{zb})\right) \\ q_1 + \frac{dt}{2} * \left(-q_0(\omega_x - \omega_{xb}) - q_3\left(\omega_y - \omega_{yb}\right) - q_2(\omega_z - \omega_{zb})\right) \\ q_2 + \frac{dt}{2} * \left(-q_3(\omega_x - \omega_{xb}) - q_0\left(\omega_y - \omega_{yb}\right) - q_1(\omega_z - \omega_{zb})\right) \\ q_3 + \frac{dt}{2} * \left(q_2(\omega_x - \omega_{xb}) - q_1\left(\omega_y - \omega_{yb}\right) - q_0(\omega_z - \omega_{zb})\right) \\ \omega_{xb} \\ \omega_{yb} \\ \omega_{zb} \end{bmatrix} \quad (10)$$

The Jacobian can then be calculated to produce matrix $F$

$$\frac{\partial f}{\partial x} = F = \begin{bmatrix} 1 & -\frac{dt}{2}(\omega_x - \omega_{xb}) & -\frac{dt}{2}\left(\omega_y - \omega_{yb}\right) & -\frac{dt}{2}(\omega_z - \omega_{zb}) & \frac{dt}{2}q_1 & \frac{dt}{2}q_2 & \frac{dt}{2}q_3 \\ \frac{dt}{2}(\omega_x - \omega_{xb}) & 1 & -\frac{dt}{2}(\omega_z - \omega_{zb}) & \frac{dt}{2}\left(\omega_y - \omega_{yb}\right) & -\frac{dt}{2}q_0 & -\frac{dt}{2}q_3 & \frac{dt}{2}q_2 \\ \frac{dt}{2}\left(\omega_y - \omega_{yb}\right) & \frac{dt}{2}(\omega_z - \omega_{zb}) & 1 & -\frac{dt}{2}(\omega_x - \omega_{xb}) & \frac{dt}{2}q_3 & -\frac{dt}{2}q_0 & -\frac{dt}{2}q_1 \\ \frac{dt}{2}(\omega_x - \omega_{xb}) & -\frac{dt}{2}\left(\omega_y - \omega_{yb}\right) & \frac{dt}{2}(\omega_x - \omega_{xb}) & 1 & -\frac{dt}{2}q_2 & \frac{dt}{2}q_1 & -\frac{dt}{2}q_0 \\ 0 & 0 & 0 & 0 & 1 & 0 & 0 \\ 0 & 0 & 0 & 0 & 0 & 1 & 0 \\ 0 & 0 & 0 & 0 & 0 & 0 & 1 \end{bmatrix} \quad (11)$$

The measurement model $h(x)$ serves to map the current state estimate $x$ onto the measurement vector y, effectively allowing the prediction to be compared with real-world measurements. Hence, this involves describing what the accelerometer and magnetometer should be reading given the current quaternion prediction, so the measurement vector can be defined as:

$$y = [a_x \quad a_y \quad a_z \quad m_x \quad m_y \quad m_z]^T \quad (12)$$

where $a_x, a_y, a_z$ are acceleration in three directions and $m_x, m_y, and\ m_z$ are magnetometer outputs.

The fixed frame gravity vector rotates into the body frame, represented by the unit quaternion q, mapping it into the accelerometer vector. This application only cares about the direction of the gravity vector and not its magnitude, so the vector is normalized before being operated on.

$$\begin{bmatrix} a_x \\ a_y \\ a_z \end{bmatrix} = h(x_k) = R(q) * \vec{g} = R(q) * \begin{bmatrix} 0 \\ 0 \\ -1 \end{bmatrix} = \begin{bmatrix} -2(q_1q_3 - q_0q_2) \\ -2(q_2q_3 - q_0q_1) \\ -q_0^2 + q_1^2 + q_2^2 - q_3^2 \end{bmatrix} \quad (13)$$

where

$$R = \begin{bmatrix} q_0^2 + q_1^2 - q_2^2 + q_3^2 & 2(q_1q_2 + q_0q_3) & 2(q_1q_3 + q_0q_2) \\ 2(q_1q_2 - q_0q_3) & q_0^2 + q_1^2 + q_2^2 - q_3^2 & 2(q_2q_3 + q_0q_1) \\ 2(q_1q_3 + q_0q_2) & 2(q_2q_3 - q_0q_1) & q_0^2 - q_1^2 - q_2^2 + q_3^2 \end{bmatrix} \quad (14)$$

Two quaternion products can be combined to form a rotation matrix R(q).

Magnetometer mapping is performed in the same way as with the accelerometer rotating the reference frame magnetic field strength vector $b$, into the body frame represented by the estimated quaternion.

where

$$\begin{bmatrix} m_x \\ m_y \\ m_z \end{bmatrix} = h(x_k) = R(q).\begin{bmatrix} b_x \\ b_y \\ b_z \end{bmatrix} = \begin{bmatrix} b_x(q_0^2 + q_1^2 - q_2^2 - q_3^2) + 2b_y(q_1q_2 + q_0q_3) + 2b_z(q_1q_3 + q_0q_2) \\ 2b_x(q_1q_2 + q_0q_3) + 2b_y(q_0^2 + q_1^2 - q_2^2 - q_3^2) + 2b_z(q_2q_3 + q_0q_1) \\ 2b_x(q_1q_3 + q_0q_2) + 2b_y(q_2q_3 + q_0q_1) + 2b_z(q_0^2 + q_1^2 - q_2^2 - q_3^2) \end{bmatrix} \quad (15)$$

These two mapping can then be combined to form the full transition function. $h(x_k)$ is presented as follows

$$h(x_k) = \begin{bmatrix} -2(q_1q_3 - q_0q_2) \\ -2(q_2q_3 - q_0q_1) \\ -q_0^2 + q_1^2 + q_2^2 - q_3^2 \\ b_x(q_0^2 + q_1^2 + q_2^2 - q_3^2) + 2b_z(q_1q_3 - q_0q_2) \\ 2b_x(q_1q_3 - q_0q_2) + 2b_z(q_2q_3 + q_0q_1) \\ 2b_x(q_1q_3 + q_0q_2) + b_z(q_0^2 + q_1^2 - q_2^2 + q_3^2) \end{bmatrix} \quad (16)$$

An attitude quaternion can be converted into Euler angles in the Tait-Bryan YPR (yaw pitch roll) order using

$$yaw = arctan\left(2.(q_0q_3 + q_1q_2), 1 - 2.(q_2^2 + q_3^2)\right)$$

DOI: 10.22034/tjee.2023.57843.4683

$$pitch = arctan\left(2.(q_0q_1 + q_2q_3), 1 - 2.(q_1^2 + q_2^2)\right)$$
$$roll = arcsin\left(2(q_0q_2 - q_3q_1)\right) \quad (17)$$

*4.2. Magnetometer Calibration*

Inexpensive electronic sensors used for measuring magnetic fields are prone to errors caused by sensor construction and the ambient field. To address this, a mean square method was employed to calibrate a triaxial magnetometer, as described in articles [8, 27, and 28]. The results of this calibration are shown in Fig. 1, which depicts three-dimensional positioning and perspective cross-sections of the measurements. Fig. 2, on the other hand, shows the 3D position and cross-sections of the calibrated data.

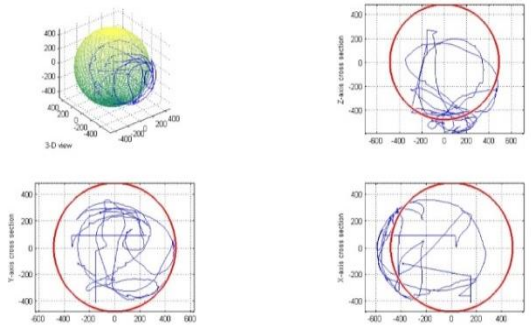

Fig. 1. 3D position and cross sections of calibrated data.

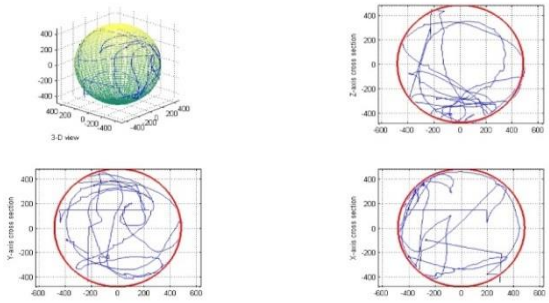

Fig. 2. Three-dimensional positioning and perspective cross-section of measurements.

*4.3. Experimental Verification*

This section evaluates the performance of the proposed approach using real data collected from a test bed, as illustrated in Fig 3. In this section, the following parameters are used:

For this simulation, the initial values of states are considered as $x_0 = [0 \quad 0 \quad 0 \quad 0 \quad 0 \quad 0 \quad 0]^T$ and the initial value of the state estimation is considered zero. The real noise power affecting the system is considered as Gaussian white noise with covariance matrices $Q = 10^{-6}I$ and $R$. Since the modeling is done in a hybrid way, two time parameters are considered T= 0.01 is the sampling time and $dt = 5 \times 10^{-3}$, which is actually the smallest time step for the continuous part.

In Algorithms 1 and 2, Robbins-Monro coefficients are used to estimate the parameter, which is considered as the initial value of the parameter $\alpha = 0.5$.

The three degrees of freedom table is used to calculate the difference between the estimated and actual status values.

**5. Conclusion**

Initial alignment is a critical issue for an inertial navigation system. The essential goal is to determine the matrix between the body and the navigation device. Kalman filter is a common technique to solve the alignment problem, but in cases where the error angle is small. If this error is large,

The designed algorithms are used to estimate the deviation and side angles, and the resulting error estimation is depicted in Fig. 4.

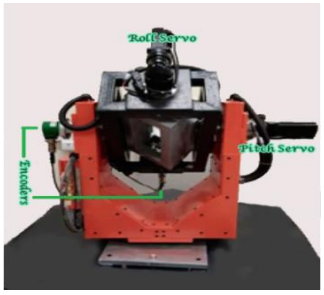


Fig. 3. Physical map of three-axis turntable testing.

A comparison of estimation Minimum Mean Squared Error (MMSE) values for designed algorithms is given in Table I. Mean Squared Error (Minimum MMSE) statistical criterion was used to evaluate the accuracy of the estimation.

Table 1. Comparison of estimation Minimum Mean Squared Error (MMSE) values for designed algorithms.

| | ROLL | PITCH | YAW |
|---|---|---|---|
| HEKF | 1.006 | 1.418 | 74.361 |
| HREKF | 0.400 | 0.516 | 20.600 |

As seen in Figure 4 and Table 1, HREKF performed much better than HEKF. It has performed very well, especially in the yaw direction. Meanwhile, the estimation of YAW values in other algorithms is not reliable. In Figure 4, the values of roll and pitch are considered zero, and the actual values of yaw are also a pseudo-triangular diagram, which is displayed in red color in the third diagram. The high performance of HREKF is evident. In the direction of ROLL and PITCH, this accuracy is improved.

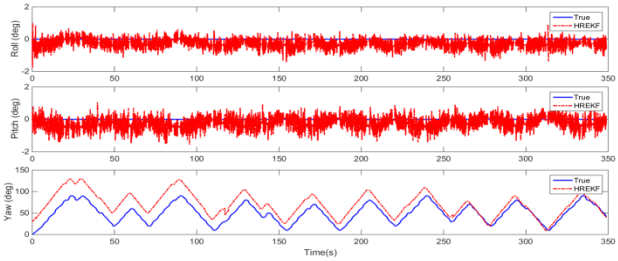


Fig. 4. Error estimation of deviation and side angles with the designed algorithms.

Additionally, the gyroscope bias is continuously estimated using parameter estimation. The validated values of the gyroscope bias are shown in Fig. 5.

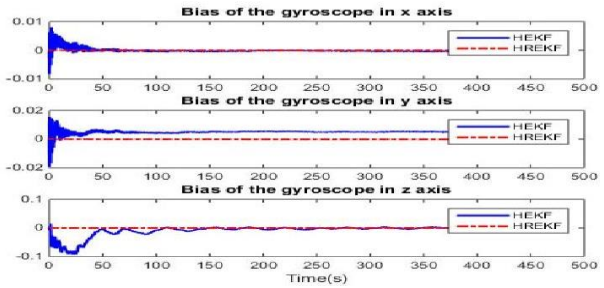

DOI: 10.22034/tjee.2023.57843.4683

the model is non-linear and a non-linear filter should be used. Since the phenomena in nature are continuous and on the other hand the output of the sensors is discrete, all the filters are modeled in a hybrid way and this work has an important contribution in modeling the system more fully and as a result having less error. But despite the successes, HEKF has linearization error and causes cumulative error. Also, YAW does not follow HEKF and therefore causes divergence. In this paper, a new algorithm called HREKF was presented. The proof of the stability of this system on the one hand and its better results in simulation based on real data on the other hand, both of which are innovations of this article, show that HREKF has a much better performance, especially in the direction of YAW, compared to HEKF. This new algorithm is not only resistant to process and system noises but also insensitive and resistant to unknown inputs and modelling uncertainties. In addition to less structural complexity, this proposed algorithm has a more effective performance in estimating the YAW direction and removing the disturbance.

## 6. Appendix

(Proof of Theorem 1)

For the stability analysis, the following assumptions and definitions have been used. Consider that, we have used it for stability analysis of the system $(A-1)$.

$$\begin{cases} \dot{x}(t) = f(x,u,t)dt + g(x,u,t)\omega(t) & t \in \mathbb{R}_{t_0}^{+} \setminus t_k \\ x(t) = h\big(\hat{x}(t_k^-), u(t_k^-)\big) & t = t_k \end{cases} \quad (A-1)$$

Eq. $(A-1)$ has been written in a general form and Eq. (1) is a special case of this form.

Some definitions

The following definitions are necessary to give the stability conditions.

**Definition 1 [30]:** Given any $C^{2,1}$ function $V: \chi \times \mathbb{R}_{t_0}^{+} \to \mathbb{R}^{+}$, the differential operator $\mathcal{L}$ associated with the continuous stochastic equation stated above, is defined as

$$\mathcal{L}V(x,t) := \frac{\partial V(x,t)}{\partial t} + \frac{\partial V(x,t)}{\partial t} f(t,x,u) + \frac{1}{2}\Big[g^T(t,x,u)\frac{\partial^2 V(x,t)}{\partial x^2} g(t,x,u)\Big].$$

By Itô 's formula in Hu et. al. [29], It obtained that

$$dV(x,t) = \mathcal{L}V(x,t)dt + \frac{\partial V(x,t)}{\partial t} g(t,x,u)d\omega(t) \qquad t \in \mathbb{R}_{t_0}^{+} \setminus t_k$$

**Definition 2 [25]**: A $C^{2,1}$ function $V: \chi \times \mathbb{R}_{t_0}^{+} \to \mathbb{R}^{+}$ is called an SISS-Lyapunov function, if there exist $\alpha_1, \alpha_2, \rho \in k_\infty, \psi \in \mathcal{P}$ such that for all $x(t_0) \in \chi, u \in U$

$$\alpha_1(|x|) \le V(x,t) \le \alpha_1(|x|) \qquad t \in \mathbb{R}_{t_0}^{+}$$

$$|x| \ge \rho(\|u\|) \Longrightarrow \begin{cases} \mathcal{L}V(x,t) \le -\hat{x}_k\big(V(x,t)\big) & t \in \mathbb{R}_{t_0}^{+} \setminus t_k \\ V(h((x,t),t) \le \psi\big(V(x,t)\big) & t = t_k \end{cases}$$

where $\mathcal{P}$ denotes the set of the functions and $\chi$ and $U$ are initial and input spaces, respectively.

We define the range of $\mathcal{T}$ as $\mathcal{T} = \{t_1, t_2, t_3, \dots\}$, where $t_k$ are the measurement times. We need the following definition. Consider following impulsive dynamic

$$\begin{cases} \dot{e}(t) = f(x,u,t) + \omega(t) & t \ne t_k \\ e(t_k^+) = e(t_k^-) - K_k\Big(y_k - h\big(\hat{x}(t_k^-)\big)\Big) & t = t_k \end{cases} \quad (A-2)$$

Now, consider following an impulsive system [30] which

Theorem A.1 [25]: Consider impulsive stochastic nonlinear system (A-1). Suppose $V: \chi \times \mathbb{R}_{t_0}^{+} \to \mathbb{R}^{+}$ is a SISS-Lyapunov function for $(A-1)$, where $\phi \in P$ is convex and $\psi \in P$ is concave. If there is certain $T, \delta > 0$ such that for all $a > 0$,

$$\int_a^{\psi(a)} \frac{ds}{\varphi(s)} \le T - \delta \quad (A-3)$$

Then, the system $(A-1)$ is SISS for all impulsive time sequences where $t_{k+1} - t_k \ge T$.

Proof of Theorem 1

Consider system $(A-1)$ and Theorem A.1. By selecting Lyapunov function $V(e,t) = \frac{1}{2}e^T P e$ we have that $\frac{1}{2}\lambda_{min}(P)e^T e \le V(e,t) \le \frac{1}{2}\lambda_{max}(P)e^T e$. So the first condition of Definition4 is established. Now, we need to check the second condition of Definition 4.

$$\mathcal{L}V(x,t) = e^T P f(x,t) + g^T(x,t)Pg(x,t) - e^T P f(\hat{x},t) - g^T(\hat{x},t)\hat{g}(x,t) \quad (A-4)$$

The function $f(.)$ satisfies the Lipshitz condition that's mean $\|f(x,t) - f(\hat{x},t)\|^2 \le \lambda\|x - \hat{x}\|^2 = \lambda\|e\|^2$ where $\lambda$ is a positive scalar value. In general, we have $g^T P g \le \lambda_{max}(P)\|g\|^2$, $\hat{g}^T P \hat{g} \le \lambda_{max}(P)\|\hat{g}\|^2$. A basic condition is $e^T P f(x,t) - e^T P f(\hat{x},t) \le -\varphi(e^T, e)$. Now, we have

$$e(t_k^-) - K_k\Big(y_k - h\big(\hat{x}(t_k^-)\big)\Big)^T p(e(t_k^-) - K_k(y_k - h(\hat{x}(t_k^-))) \le \psi(v(x,t))^T \quad (A-5)$$

So, by setting conditions of Definition 4 and assuming $\int_a^{\psi(a)} \frac{ds}{\varphi(s)} \le T - \delta$ in Theorem A.1, the system is stochastic global stability. Now, assuming $\varphi = cV\,(e,t)$ and $\psi = e^{-d}V(e,t)$, we have $\mathcal{L}V(x,t) = e^T P f(x,t) - e^T P f(\hat{x},t) \le -ce^T Pe$.

This equation indicates the dynamic of continuous of systems without impulses is stochastic global stability. Since we assumed the stability of the continuous system, no need to check it. Now, consider the second condition of (11) at impulsive instances.

$$V(h\big((x,t),t\big) = (e(t_k^-) - K_k(y_k - h(\hat{x}(t_k^-))^T P(e(t_k^-) - K_k(y_k - h\big(\hat{x}(t_k^-)\big))) \le e^{-d}e^T Pe(t_k) \quad (A-6)$$

We set, $e(t_k^-) = e$, so

$$e^T(P - e^{-d}P)e + 2e^T PK_k(y_k - h\big(\hat{x}(t_k^-)\big) + K_k(y_k - h\big(\hat{x}(t_k^-)\big)^T PK_k(y_k - h\big(\hat{x}(t_k^-)\big)) < \quad (A-7)$$

In the above relation, the inequality $2x^T y \le \epsilon\, x^T x + \epsilon^{-1}y^T y$ is used. So, we use an inequality matrix:

$$V(h\big((x,t),t\big) \le e^T(P - e^{-d}P)e + \epsilon e^T PK_k K_k^T P + \epsilon^{-1}\big(y - h(t_k^{-1})\big)^T\Big(y - h\big(x(t_k)\big)\Big) \quad (A-8)$$

In the above relation $\big(y - h(t_k^{-1})\big)^T\Big(y - h\big(x(t_k)\big)\Big) \le \eta e^T e$ should be used which arises from the Lipshitz condition. So, we have $e^T(P - e^{-d}P + \epsilon pK_k K_k^T + \epsilon^{-1}\eta I)e < 0$. Since the main dynamics is continuous, and using Shcur compliment, then $d < 0$ and

$$\begin{bmatrix} (e^{-d}-1)P & PK_k & I \\ K_k^T P^T & \epsilon^{-1}I & 0 \\ I & 0 & \epsilon\eta^{-1}I \end{bmatrix} > 0 \quad (A-9)$$

$P > 0$ (Symmetric positive matrix) and $\epsilon > 0$ (scalar) then condition

$$\int_a^{e^{-d}a} \frac{1}{v}dv = \frac{1}{c}\ln v\,\Big|_a^{e^{-d}a} = \frac{1}{c}(\ln e^{-d}a - \ln a) = \frac{\ln e^{-d}}{c} = -\frac{d}{c} \le T - \delta \quad (A-10)$$

So, we have $T > -\frac{d}{c} + \delta$. The proof is completed.

**Remark 3**: Note that Theorem A.1 is a general theorem. If we compare with the form of system (1), we see that the function $g(x, u, t)$ is equal to the unit function in system (1) and this system is a special firm of $(A - 1)$ with $g(x, u, t) = I$. Therefore, without losing the principle of the problem, we advanced the proof in a general way, until we see that the function $g(x, u, t)$ satisfies the conditions of the problem ($g^T P g \leq \lambda_{max}(P)\|g\|^2$). Therefore, the function $g(x, u, t)$ does not appear in the final results.

**7.Acknowledgment**
The authors would like to thank the associate editor and the anonymous reviewers for their valuable comments and constructive suggestions. They were very helpful for this study. We also thank the Laboratory of Instrumentation of the University of Science and Technology for their cooperation.

**8. References**

[1] S. Ashraf, P. Aggarwal, P. Damacharla, "A low-cost solution for unmanned aerial vehicle navigation in a global positioning system–denied environment", *International Journal of Distributed Sensor Networks*, vol. 14, no. 6, 2018.

[2] V.H.A. Ribeiro, R. Santana, G. Reynoso-Meza, "Random vector functional link forests and extreme learning forests applied to UAV automatic target recognition", *Engineering Applications of Artificial Intelligence*, vol. 117, article no. 105538, 2023.

[3] M. Gunia, Y. Wu, N. Joram, F. Ellinger, "Building up an inertial navigation system using standard mobile devices", *Journal of Electrical Engineering*, vol. 5, pp. 299-320, 2017.

[4] M.T. Sabet, H.M. Daniali, A. Fathi, "A low-cost dead reckoning navigation system for an AUV using a robust AHRS: Design and experimental analysis", *IEEE Journal of Oceanic Engineering*, vol. 43, no. 4, pp. 927-939, 2017.

[5] P.K. Yoon, S. Zihajehzadeh, B.S. Kang, "Robust biomechanical model-based 3-D indoor localization and tracking method using UWB and IMU", *IEEE Sensors Journal*, vol. 17, no. 4, pp. 1084-96, 2014.

[6] W. Li, J. Wang, "Effective adaptive Kalman filter for MEMS-IMU/magnetometers integrated attitude and heading reference systems", *The Journal of Navigation*, vol. 66, no. 1, pp. 99-113, 2013.

[7] Y. Liu, X. Xu, X. Liu, "A self-alignment algorithm for SINS based on gravitational apparent motion and sensor data denoising", *Sensors*, vol. 15, no. 5, pp. 9827-53, 2015.

[8] D. Titterton, J.L. Weston, J. Weston, "Strapdown inertial navigation technology", *IET*, 2004.

[9] R. Munguía, A. Grau, "A practical method for implementing an attitude and heading reference system", *International Journal of Advanced Robotic Systems*, vol. 11, no. 4, pp. 62, 2014.

[10] L. Chang, F. Zha, F. Qin, "Indirect Kalman filtering based attitude estimation for low-cost attitude and heading reference systems", *IEEE/ASME Transactions on Mechatronics*, vol. 22, no. 4, pp. 1850-1858, 2017.

[11] J.K. Lee, M.J. Choi, "A sequential orientation Kalman filter for AHRS limiting effects of magnetic disturbance to heading estimation", *Journal of Electrical Engineering Technology*, vol. 12, pp. 1675-1682, 2017.

[12] F. Yin, L. Wang, W. Tian, X. Zhang, "Kinematic calibration of a 5-DOF hybrid machining robot using an extended Kalman filter method", *Precision Engineering*, vol. 79, pp. 86-93, 2023.

[۱۳] م، مجیدی، ع، عرفانیان، ح، خالوزاده، "مقاوم‌سازی موقعیت‌یابی در برابر فریب GPS با استفاده از سامانه‌های INS و Loran-C. *مجله مهندسی برق دانشگاه تبریز*، دوره ۴۸،شماره پیاپی ۸۵، صفحه ۱۳۶۵-۱۳۷۷

[14] X. Kai, L. Liangdong, L. Yiwu, "Robust extended Kalman filtering for nonlinear systems with multiplicative noises", *Optimal Control Applications and Methods*, vol. 32, no. 1, pp. 47-63, 2011.

[15] X. Kai, C. Wei, L. Liu, "Robust extended Kalman filtering for nonlinear systems with stochastic uncertainties", *IEEE Transactions on Systems, Man, and Cybernetics-Part A: Systems and Humans*, vol. 40, no. 2, pp. 399-405, 2009.

[16] B. Candan, H.E. Soken, "Robust attitude estimation using IMU-only measurements", *IEEE Transactions on Instrumentation and Measurement*, vol. 70, pp. 1-9, 2021.

[17] D.A. Aligia, B.A. Roccia, C.H. De Angelo, G.A. Magallan, G.N. Gonzalez, "An orientation estimation strategy for low cost IMU using a nonlinear Luenberger observer", *Measurement*, vol. 173, article no. 108664, 2021.

[18] T. Du, L. Guo, J. Yang, "A fast initial alignment for SINS based on disturbance observer and Kalman filter", *Transactions of the Institute of Measurement and Control*, vol. 38, no. 10, pp. 1261-1269, 2016.

[19] J. Sun, X.S. Xu, Y.T. Liu, "Initial alignment of large azimuth misalignment angles in SINS based on adaptive UPF", *Sensors*, vol. 15, no. 9, pp. 21807-21823, 2015.

[20] S.P. Dmitriyev, O.A. Stepanov, S.V. Shepel, "Nonlinear filtering methods application in INS alignment", *IEEE Transactions on Aerospace and Electronic Systems*, vol. 33, no. 1, pp. 260-272, 1997.

[۲۱] ع.علما، م، شاصادقی،ا، رمضانی، "طراحی کنترل‌کننده پیش‌بین مدل پایدارساز برای سیستم‌های هایبرید مرکب منطقی دینامیکی: رویکرد تابع لیاپانف مبتنی بر نُرم بی‌نهایت"، *مجله مهندسی برق، دانشگاه تبریز*، دوره۵۰،شماره ۴،صفحه ۱۷۳۴-۱۷۴۴.

[22] K. Masuya, T. Sugihara, "A nonlinear complementary filter for attitude estimation with dynamics compensation of MARG sensor", *in Proceedings of the 2016 IEEE International Conference on Advanced Intelligent Mechatronics* (AIM), pp. 976-981, 2016.

[23] Y.C. Fan, Y.H. Tseng, C.Y. Wen, "A Novel Deep Neural Network Method for HAR-Based Team Training Using Body-Worn Inertial Sensors", *Sensors*, vol. 22, no. 21, article no. 8507, 2022.

[24] D. Simon, "Optimal state estimation: Kalman, H infinity, and nonlinear approaches", John Wiley & Sons.

[25] W. Ren, J. Xiong, "Stability analysis of impulsive stochastic nonlinear systems", IEEE Transactions on Automatic Control, vol. 62, no. 9, pp. 4791-4797, 2017.

[26] Liguang Xu, Shuzhi Sam Ge & Hongxiao Hu, "Boundedness and stability analysis for impulsive stochastic differential equations driven by G-Brownian motion", International, Journal of Control, 92:3, 642-652, 2019.

[27] L.C.G. Rogers, D. Williams, "Diffusions, Markov processes and martingales", Volume 2, Itô calculus, Cambridge University Press, 2000.

[28] M. Kok, J.D. Hol, T.B. Schön, "Calibration of a magnetometer in combination with inertial sensors", *in Proceedings of the 2012 15th International Conference on Information Fusion*, pp. 787-793, 2012.

DOI: 10.22034/tjee.2023.57843.4683

[29] X. Mao, "Stochastic Differential Equations and Applications", 2nd ed., *Elsevier, Chichester*, U.K, Horwood, 2007.

[30] L. Hu, X. Li, X. Mao, "Convergence rate and stability of the truncated Euler-Maruyama method for stochastic differential equations", *Journal of Computational and Applied Mathematics*, vol. 337, pp. 274-289, 2018.